• Basic Research •

MSH6 gene methylation on clinical pathology and diagnosis in retinoblastoma: a bioinformatics analysis

Cheng-Fang Zhang[1], *Liang Zhao*[2], *Tian-Ming Jian*[2], *Yu-Feng Guo*[1]

[1]Department of Ophthalmology, Tianjin Hospital, Tianjin 300211, China
[2]Department of Orbital Disease and Oculoplastic Surgery, Tianjin Key Laboratory of Retinal Functions and Diseases, Tianjin Branch of National Clinical Research Center for Ocular Disease, Eye Institute and School of Optometry, Tianjin Medical University Eye Hospital, Tianjin 300384, China
Correspondence to: Liang Zhao. Department of Orbital Disease and Oculoplastic Surgery, Tianjin Key Laboratory of Retinal Functions and Diseases, Tianjin Branch of National Clinical Research Center for Ocular Disease, Eye Institute and School of Optometry, Tianjin Medical University Eye Hospital, Tianjin 300384, China. liangzhaoeye83@163.com
Received: 2025-02-14 Accepted: 2025-08-12

Abstract

• **AIM:** To explore the methylation status of *MSH6* in retinoblastoma (RB) and its impact on clinicopathological features and diagnosis.

• **METHODS:** Differentially expressed genes were identified through bioinformatics screening of the GSE24673 and GSE125903 datasets, combined with GeneCards database analysis. A total of 102 RB patients and 62 trauma-enucleated controls between January 2018 and December 2023 were enrolled, with their clinicopathological data and retinal tissues collected. The mRNA and methylation levels of *MSH6* in retinal tissues were detected using real-time quantitative polymerase chain reaction (PCR) and methylation-specific PCR. Western blot analysis was conducted in one pair of RB and control tissues for preliminary protein-level validation of MSH6 expression. Based on the methylation status of *MSH6*, RB patients were categorized into two groups: low-methylation and high-methylation. Both univariate and multivariate analyses were conducted to identify independent factors influencing the methylation levels using clinicopathological data. Receiver operating characteristic (ROC) curves were applied to evaluate the diagnostic potential of *MSH6* methylation in RB.

• **RESULTS:** Bioinformatics analysis of public datasets revealed that MSH6 expression was downregulated across multiple cancers, RB. Consistently, in clinical RB tissues, *MSH6* mRNA expression was significantly lower than that in control retinal tissues, whereas the promoter methylation level of *MSH6* was markedly higher (both $P<0.001$), indicating that promoter hypermethylation may contribute to transcriptional silencing of *MSH6* in RB. Patients with higher *MSH6* methylation levels showed more advanced pathological classification and a higher frequency of metastasis. Multivariate logistic regression confirmed that metastatic status ($P=0.008$, OR=3.51) and pathological classification ($P=0.005$, OR=3.7) were independent factors associated with MSH6 methylation. Receiver operating characteristic (ROC) analysis demonstrated that *MSH6* methylation could effectively distinguish RB tissues from non-tumorous controls (AUC=0.847, sensitivity=78.43%, specificity=80.65%), suggesting that *MSH6* hypermethylation may serve as a potential diagnostic biomarker for RB.

• **CONCLUSION:** The methylation level of the *MSH6* gene may be a key factor in RB pathogenesis. The methylation status of the *MSH6* gene is closely associated with clinicopathological features and shows diagnostic potential.

• **KEYWORDS:** retinoblastoma; *MSH6*; diagnosis; methylation; clinical pathology

DOI:10.18240/ijo.2025.12.05

Citation: Zhang CF, Zhao L, Jian TM, Guo YF. *MSH6* gene methylation on clinical pathology and diagnosis in retinoblastoma: a bioinformatics analysis. *Int J Ophthalmol* 2025;18(12):2255-2262

INTRODUCTION

Retinoblastoma (RB), the most common intraocular malignant tumor in childhood, is typically diagnosed in children under 5 years old and represents approximately 3% of all pediatric cancers[1]. While the survival rate of RB has significantly improved with early diagnosis and therapeutic advances, high mortality rates still persist in high-risk patients, especially those with late-stage or metastatic disease[2-3]. Consequently, accurate early identification of high-risk individuals and implementation of personalized therapeutic strategies remain critical research priorities in RB management.

As a classically hereditary malignancy, RB is closely associated with mutations in the *RB1* tumor suppressor gene, which is located on chromosome 13q14. Mutations in this gene lead to abnormal proliferation of retinal cells, resulting in tumor formation[4]. Although *RB1* mutations are the primary pathogenic mechanism of RB, an increasing number of studies have shown that the occurrence and progression of the tumor involve complex interactions with additional genetic and molecular pathways. Epigenetic dysregulation, particularly aberrant DNA methylation, has emerged as a key contributor to RB pathogenesis[5]. DNA methylation is an important epigenetic modification that regulates gene expression and plays well-established roles in cancer onset, progression, and drug resistance[6]. Therefore, characterizing DNA methylation alterations in RB and their impacts on clinicopathological features and prognosis is crucial for advancing diagnostic and therapeutic approaches.

MSH6 (MutS homolog 6) is a key component of the DNA mismatch repair system, responsible for repairing mismatches that occur during DNA replication[7]. Both the *MSH6* gene and its protein product are critical for maintaining genomic stability through DNA damage repair. Functional impairment or abnormal expression of *MSH6* compromises DNA repair capacity, thereby promoting tumorigenesis and tumor progression. Deletion, mutation, or downregulation of the *MSH6* gene demonstrates established associations with the development of multiple malignancies, including colorectal, gastric, and lung cancers[8-9]. Notably, abnormal methylation of the *MSH6* gene has been found to be linked to the occurrence and prognosis of these tumors, suggesting its utility as an early diagnostic marker or prognostic factor[10]. Despite this evidence, the role of *MSH6* in RB remains underexplored, with no systematic studies reported to date.

In this study, we combined multi-omics data from the Gene Expression Omnibus (GEO) database to identify differentially expressed genes (DEGs) closely associated with RB development and progression through bioinformatics methods. Focusing on *MSH6*, we subsequently characterized its expression patterns and methylation status. Using real-time quantitative polymerase chain reaction (qPCR) and methylation-specific PCR (MSP), *MSH6* expression and methylation levels were validated in clinical RB specimens, and their correlations with clinicopathological features were analyzed. By integrating bioinformatics analysis with clinical validation, this study aims to elucidate the potential role of *MSH6* gene methylation in RB pathogenesis and to explore its value as a diagnostic biomarker.

PARTICIPANTS AND METHODS

Ethical Approval The study received approval from Tianjin Medical University Eye Hospital's Medical Ethics Committee [No.2024KY(L)-18], and informed consent was obtained from the guardians of all children involved in the study.

Study Design This study included 102 children with RB who underwent surgical treatment at the Department of Ophthalmology, Tianjin Medical University, between January 2018 and December 2023. The cohort consisted of 59 males and 43 females. Inclusion criteria were: 1) diagnosis of RB according to established criteria[11], with confirmation by postoperative pathological examination; 2) complete clinical records with no missing data; 3) unilateral disease. Exclusion criteria included: 1) concurrent hematological disorders; 2) additional malignant tumors; 3) abnormal function of organs such as the heart and liver; 4) patients who refused or did not complete relevant examinations. In addition, 62 children undergoing enucleation due to traumatic indications with histologically confirmed normal retinal tissues were selected as the control group. These children exhibited no evidence of tumor-related diseases upon comprehensive examination, with 37 males and 25 females. No notable difference was observed in the basic characteristics between the two groups (P>0.05), ensuring comparability.

Methods

Bioinformatics analysis Datasets GSE24673 and GSE125903 related to RB were retrieved from the GEO database (https://www.ncbi.nlm.nih.gov/gds/). DEGs were identified by comparing the gene expression profiles of RB samples with normal retinal controls. Protein interaction data were downloaded from GeneCards (https://www.genecards.org/), with DEG intersections visualized using the Jvenn system (https://jvenn.toulouse.inrae.fr/app/example.html). The prognostic significance of candidate DEGs across various cancers was analyzed *via* the Kaplan-Meier plotter platform (https://kmplot.com/analysis/).

Clinical data Demographic and clinicopathological characteristics of all RB patients were collected, including age, gender, lesion site, optic nerve involvement, metastatic status, chemotherapy history, and pathological classification.

Quantitative polymerase chain reaction Following the manufacturer's instructions, TRIzol reagent (15596026CN, Invitrogen, CA, USA) was used to extract total RNA from retinal tissues. The purity and concentration of the extracted RNA were measured using a NanoDrop One spectrophotometer. RNA was then reverse transcribed into cDNA using the RevertAid cDNA Synthesis Kit, followed by SYBR green-based qPCR amplification, with *MSH6*-specific primers designed and synthesized by GenePharma (Shanghai) Co., Ltd. (Table 1). *MSH6* gene expression was normalized to glyceraldehyde-3-phosphate dehydrogenase (*GAPDH*) as the internal control. All qPCR reactions were performed in triplicate to ensure reproducibility, and no-template controls

were included to monitor contamination. The specificity of amplification was confirmed by melt curve analysis. After obtaining the threshold cycle (Ct) values for each sample, data were analyzed using the $2^{-\Delta\Delta Ct}$ method to calculate the fold change in target gene expression between the experimental and control groups with the formula: $\Delta\Delta Ct=(Ct_{target\ gene}-Ct_{reference\ gene})_{experimental\ group}-(Ct_{target\ gene}-Ct_{reference\ gene})_{control\ group}$.

Methylation-specific polymerase chain reaction Genomic DNA was extracted from retinal tissues using a DNA extraction kit. Extracted DNA underwent CpG methyltransferase treatment followed by bisulfite conversion using reagents purchased from Dalian TaKara Biotechnology Co., Ltd. For each reaction, 1 μg of peripheral blood-derived DNA was enzymatically modified following the instructions of the methyltransferase kit. To mitigate false negatives/positives, all samples were subjected to parallel amplification with both methylated and unmethylated primer sets. Fully methylated and unmethylated human genomic DNA (commercial standards) were included as positive controls for bisulfite conversion and MSP, while deionized water was used as a negative control. All MSP reactions were independently repeated at least twice to verify reproducibility. Additional positive controls for methylation/unmethylation status comprised CpG methyltransferase-treated DNA and bisulfite-converted retinal DNA, with deionized water serving as the negative control. Primer sequences synthesized by Shanghai Biotechnology Co., Ltd. are listed in Table 2, and experimental reagents were purchased from Dalian TaKara Biotechnology Co., Ltd.

The MSP protocol for *MSH6* (173 bp): Pre-denaturation at 95℃ for 3min, followed by 37 cycles of 94℃ for 30s, 58℃ for 20s, and 72℃ for 20s, with a final extension at 72℃ for 5min.

The unmethylation-specific PCR protocol (173 bp): Pre-denaturation at 95℃ for 3min, followed by 37 cycles of 94℃ for 30s, 56℃ for 20s, and 72℃ for 20s, with a final extension at 72℃ for 5min. PCR products were analyzed using 2% agarose gel electrophoresis.

Interpretation criteria for PCR results: Samples showing specific amplification products for the methylated primers, with or without amplification products for the unmethylated primers, were considered positive (methylated). Conversely, samples showing only amplification for the unmethylation-specific primers were considered negative (unmethylated).

Western blot Total protein was extracted from RB tissues and matched normal retinal tissues using RIPA lysis buffer (Beyotime, Shanghai, China) supplemented with protease inhibitors. Protein concentrations were determined using a bicinchoninic acid assay kit. Equal amounts (20-30 μg) of protein per sample were separated by sodium dodecyl sulfate-polyacrylamide gel electrophoresis and transferred to polyvinylidene fluoride membranes (Millipore). Membranes were blocked with 5% non-fat milk in Tris-buffered saline with Tween-20 for 1h at room temperature and incubated overnight at 4℃ with the following primary antibodies: anti-MSH6 (AB25640, 1:3000, ABclonal, Wuhan, China) and anti-GAPDH (AC001, 1:10 000, ABclonal, Wuhan, China). After washing, membranes were incubated with horseradish peroxidase-conjugated secondary antibodies (AC054, 1:5000, ABclonal, Wuhan, China) for 1h at room temperature. Protein bands were detected using enhanced chemiluminescence substrate (Thermo Fisher) and imaged with a Tanon imaging system. Densitometric analysis was performed using ImageJ software, with MSH6 expression normalized to GAPDH.

Table 1 Primer sequences for qPCR

Gene	Sequence
MSH6	F: 5′-CGGAGTCAACGGATTTGGTCGTAT-3′
	R: 5′-AGCCTTCTCCATGGTGGTGAAGAC-3′
GAPDH	F: 5′-AATGGGCAGCCGTTAGGAAA-3′
	R: 5′-GCGCCCAATACGACCAAATC-3′

qPCR: Quantitative polymerase chain reaction; *MSH6*: MutS homolog 6; *GAPDH*: Glyceraldehyde-3-phosphate dehydrogenase.

Table 2 Primer sequences for MSP

Gene	Sequence
MSH6 methylation	F: 5′-TTCGTTAGTAGGAGTCGCGC-3′
	R: 5′-TTCGCGTAAAACCCTAACCG-3′
MSH6 unmethylation	F: 5′-TTTGTTAGTAGGAGTTGTGT-3′
	R: 5′-TTCACATAAAACCCTAACCA-3′

MSP: Methylation-specific polymerase chain reaction; *MSH6*: MutS homolog 6.

Statistical Analysis Data analysis was performed using SPSS 26.0 statistical software. All statistical tests were two-tailed, with a significance threshold of $P<0.05$. The normality of continuous data was evaluated with the Shapiro-Wilk test. For comparisons between two groups, *t*-tests were employed, and normally distributed data were presented as mean±standard deviation. Univariate and binary logistic regression analyses were conducted to identify potential risk factors. Receiver operating characteristic (ROC) curves were used to evaluate the diagnostic value of *MSH6* methylation levels. The optimal cutoff value was determined by the Youden index to maximize the combined sensitivity and specificity. Additionally, the area under the curve (AUC) for each biomarker was calculated to assess its diagnostic performance.

RESULTS

DEGs in Retinoblastoma-related GEO Datasets In this study, DEG analysis was performed on RB-related GEO and GeneCards datasets, with the results presented in Figure 1A. Two datasets, GSE24673 and GSE125903, were selected, and differential gene expression between RB samples and

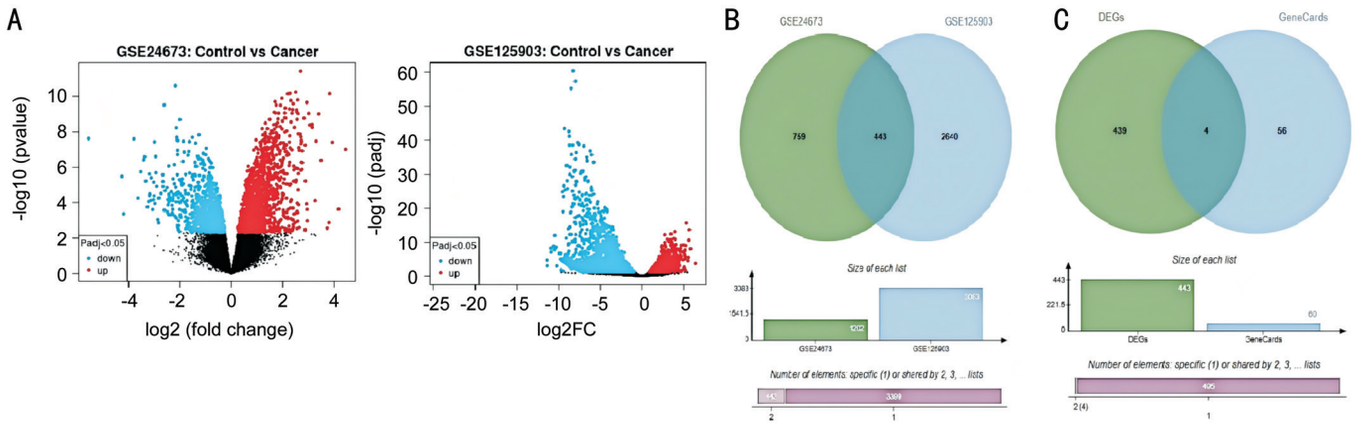

Figure 1 Screening of DEGs in RB-related datasets A: Volcano plots display the DEGs between retinoblastoma and control samples in the GSE24673 and GSE125903 datasets; B: Venn diagram depicts the common DEGs identified in both GEO datasets; C: Venn diagram shows the overlap of GEO-derived DEGs and GeneCards-retrieved retinoblastoma-associated proteins. DEGs: Differentially expressed genes; RB: Retinoblastoma; GEO: Gene Expression Omnibus.

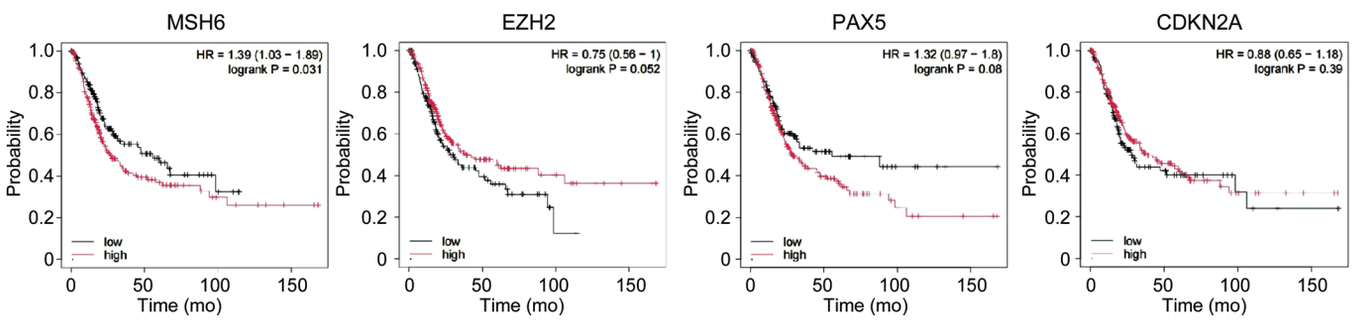

Figure 2 Prognostic significance of RB-associated DEGs in pan-cancer survival analysis RB: Retinoblastoma; DEGs: Differentially expressed genes.

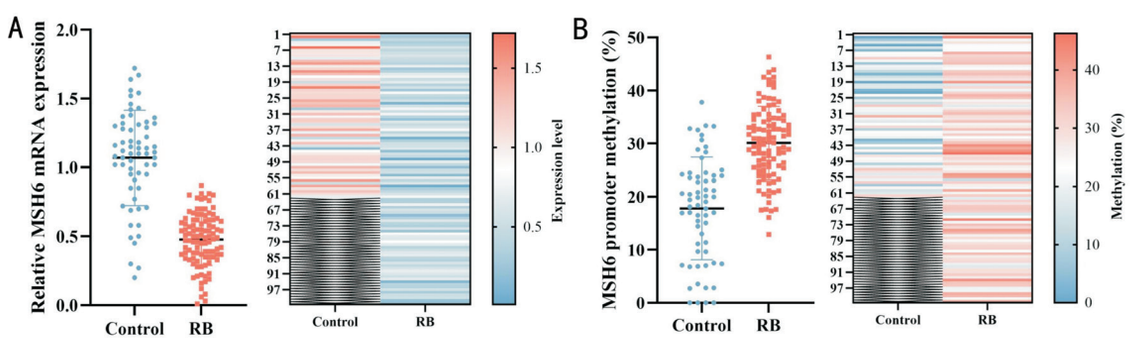

Figure 3 *MSH6* mRNA expression and methylation levels in RB tissues A: Scatter plot showing relative *MSH6* mRNA expression in control and RB tissues. Each dot represents one sample; horizontal lines indicate mean±standard deviation. Heatmap showing normalized *MSH6* mRNA expression (control, RB), color bar indicates expression level. B: Scatter plot showing *MSH6* promoter methylation (%) in control and RB tissues. Heatmap of methylation levels, with color bar representing methylation percentage. *MSH6*: MutS homolog 6; RB: Retinoblastoma.

normal controls were compared, leading to the identification of significantly dysregulated genes. A Venn diagram (Figure 1B) illustrates 443 DEGs common to both datasets. Separately, GeneCards-derived proteins associated with "RB" (relevance score >20) yielded a total of 60 RB-related candidates. Intersectional analysis of these 443 DEGs and 60 proteins identified four final RB-related targets: *MSH6*, *EZH2*, *PAX5*, and *CDKN2A*. These genes showed significant differential expression in RB samples, suggesting potential roles in of RB pathogenesis.

Analysis of *MSH6* Expression Across Multiple Cancer Types Kaplan-Meier plotter was used to analyze the survival data of the four DEGs. The results indicated that *MSH6* was significantly associated with the prognosis of pan-cancer patients (Figure 2). Based on these findings, *MSH6* was selected as the focus of subsequent studies to investigate its role in RB. Further details were in Figure 3.

***MSH6* mRNA Expression and Methylation Levels in Retinoblastoma Tissues** The expression level of *MSH6* mRNA in the control group was significantly higher than that

Table 3 Association between *MSH6* gene methylation levels and clinicopathological features in RB patients *n* (%)

Indicators	Low-methylation group (*n*=52)	High-methylation group (*n*=50)	*t*	*P*
Age, mean±SD	2.04±0.72	2.19±0.76	0.991	0.324
Gender			0.187	0.665
Male	29 (55.77)	30 (60.00)		
Female	23 (44.23)	20 (40.00)		
Lesion site			0.945	0.331
Left eye	32 (61.54)	26 (52.00)		
Right eye	20 (38.46)	24 (48.00)		
Optic nerve involvement			3.923	0.048
Yes	21 (40.38)	30 (60.00)		
No	31 (59.62)	20 (40.00)		
Metastatic status			5.944	0.015
Yes	24 (46.15)	35 (70.00)		
No	28 (53.85)	15 (30.00)		
Chemotherapy			6.713	0.010
Yes	21 (40.38)	33 (66.00)		
No	31 (59.62)	17 (34.00)		
Pathological classification			8.927	0.003
Undifferentiated type	20 (38.46)	34 (68.00)		
Differentiated type	32 (61.54)	16 (32.00)		

MSH6: *MutS homolog 6*; RB: Retinoblastoma; SD: Standard deviation.

Table 4 Independent risk factors for *MSH6* gene methylation levels in RB patients

Factor	*B*	SE	Wald χ^2 value	*P*	OR (95%CI)
Constant	-2.158	0577	13.981	<0.001	0.116
Optic nerve involvement	0.494	0.477	1.074	0.300	1.639 (0.644-4.172)
Metastatic status	1.256	0.473	7.06	0.008	3.51 (1.390-8.865)
Chemotherapy	0.794	0.481	2.725	0.099	2.213 (0.862-5.681)
Pathological classification	1.308	0.466	7.868	0.005	3.7 (1.483-9.230)

MSH6: MutS homolog 6; RB: Retinoblastoma; SE: Standard error; OR: Odds ratio; CI: Confidence interval.

in the RB group (1.07±0.35 *vs* 0.48±0.19; t=14.148, P<0.001). Conversely, the methylation level of the *MSH6* gene was significantly lower in the control group compared to the RB group (17.79±9.67 *vs* 30.10±6.91; t=9.476, P<0.001). Detailed results are shown in Figure 3.

MSH6 Protein Expression in Retinoblastoma and Control Tissues Western blot analysis of one pair of RB and normal retinal tissues showed that MSH6 protein levels were lower in the RB tissue compared to the normal control (Figure 4). Densitometric quantification revealed a decrease in the relative expression of MSH6 (normalized to GAPDH) in the RB group compared to the control group. These results are consistent with our mRNA and methylation data, collectively indicating that *MSH6* promoter methylation is associated with its downregulation at both transcriptional and protein levels in RB.

Relationship Between *MSH6* Gene Methylation Levels and Clinicopathological Features In this study, the mean *MSH6* gene methylation level of 30.10 in RB patients was used as the cutoff point, dividing the patients into low-methylation and high-methylation groups. The results indicated that *MSH6* methylation levels were significantly associated with clinicopathological features such as optic nerve involvement, metastasis, chemotherapy history, and pathological classification (Table 3).

Independent Risk Factors for *MSH6* Gene Methylation Levels in Retinoblastoma Patients Factors with statistically significant differences (optic nerve involvement, metastasis, chemotherapy, and pathological classification) identified in the previous analysis were further examined. In the multivariable logistic regression analysis, the categorical variables were coded as follows: optic nerve involvement (0=no, 1=yes), metastasis (0=no, 1=yes), chemotherapy (0=no, 1=yes), and pathological classification (0=undifferentiated type, 1=differentiated type). The results showed that metastasis and pathological classification were independent risk factors for *MSH6* methylation levels in RB patients (Table 4).

Diagnostic Value of *MSH6* Gene Methylation Levels for Retinoblastoma ROC curve analysis indicated that *MSH6* gene methylation levels in tissues exhibited significant

Table 5 Diagnostic value of *MSH6* gene methylation levels for RB

Factor	AUC	SE	95%CI	Sensitivity, %	Specificity, %	Youden's index
MSH6 gene methylation level	0.847	0.032	0.785-0.909	78.43	80.65	0.591

MSH6: *MutS homolog 6*; RB: Retinoblastoma; AUC: Area under the curve; SE: Standard error; CI: Confidence interval.

diagnostic value for RB, with an AUC of 0.847, sensitivity of 78.43%, specificity of 80.65%, and an optimal cutoff value of 0.591 (Table 5, Figure 5).

DISCUSSION

RB is a childhood intraocular malignancy where significant challenges persist despite advances in early diagnosis and treatment. High-risk patients continue to face poor prognoses due to metastasis, recurrence, and chemotherapy resistance[12]. Recent research indicates that epigenetic modifications, especially aberrant DNA methylation, play important roles in the initiation and progression of tumors, including RB[13-14]. The *MSH6* gene, a key component of the DNA mismatch repair system, has been shown to play a pivotal role in genomic stability maintenance across a variety of cancer types[15-16]. However, the specific role of *MSH6* in RB, particularly the functional significance of its methylation status, remains unclear.

MSH6 gene, located on chromosome 2p16, was first cloned in 1995 and spans 4.2 kb. It encodes a 160 kD protein that belongs to the MutS family of DNA mismatch repair proteins. *MSH6* forms a dimer with *MSH2* (hMutSα complex), which recognizes and repairs single-base mismatches and small insertion/deletion loops in DNA. Loss of normal *MSH6* function impairs DNA repair, leading to increased base mismatches. Animal studies have shown that *MSH6*-deficient mice are more likely to develop tumors, and combined *MSH6* and *p53* deficiencies accelerate tumorigenesis[17]. Abnormal expression of *MSH6* has also been linked to a variety of human cancers, including hereditary nonpolyposis colorectal cancer, prostate cancer, breast cancer, endometrial cancer, pituitary neuroendocrine tumors, glioblastoma, renal cell carcinoma, and ovarian cancer[18-23]. Nevertheless, the relationship between *MSH6* dysfunction and RB development remains largely unexplored.

Our bioinformatics analysis suggests that *MSH6* may play an important role in the pathogenesis and progression of RB. We observed that low diminished *MSH6* expression was associated with more aggressive tumor features. This observation is consistent with previous studies showing that reduced *MSH6* expression impairs DNA repair, increases genomic instability, and promotes tumor progression across multiple malignancies[18-19]. However, further studies are needed to clarify the functional impact of *MSH6* downregulation specifically in RB.

Epigenetic alterations, such as DNA methylation, are

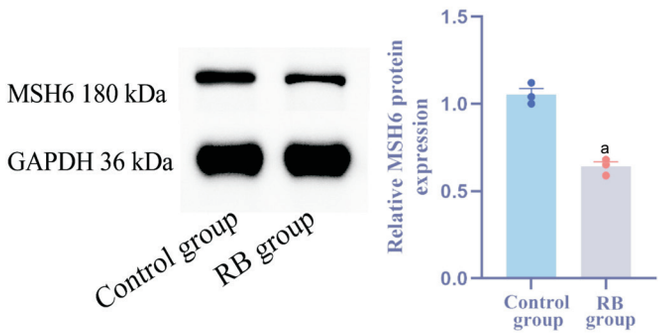

Figure 4 Western blot analysis of MSH6 protein expression in RB and normal retinal tissues Representative immunoblots for MSH6 (180 kDa) and GAPDH (36 kDa) are shown. The bar graph displays quantification of MSH6 relative to GAPDH. MSH6: MutS homolog 6; RB: Retinoblastoma; GAPDH: Glyceraldehyde-3-phosphate dehydrogenase. [a]*P*<0.001.

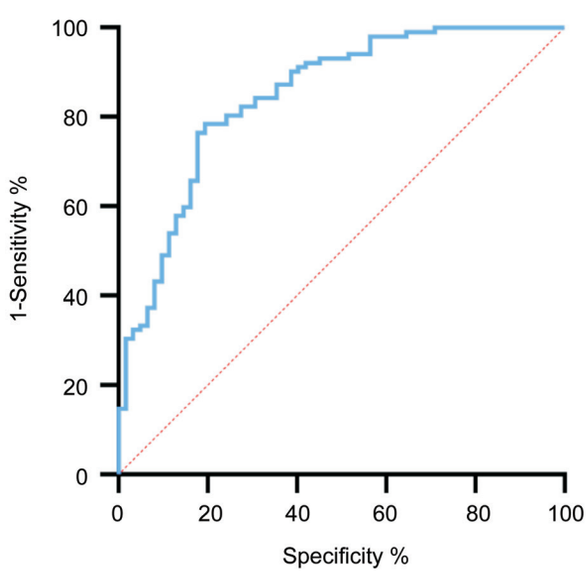

Figure 5 ROC curve analysis of the diagnostic value of *MSH6* gene methylation in RB ROC: Receiver operating characteristic; *MSH6*: MutS homolog 6; RB: Retinoblastoma.

common in tumor development. Unlike gene mutations, promoter CpG island methylation can transcriptionally silence tumor suppressor and DNA repair genes. Previous studies have reported frequent *MSH6* methylation in pituitary neuroendocrine tumors[24] and early-stage breast cancer[25], whereas such epigenetic changes are notably absent in certain glioblastomas[26]. In our study, *MSH6* methylation levels were significantly higher in RB patients than those in healthy controls. Elevated *MSH6* methylation was also associated with adverse clinicopathological features such as optic nerve involvement, metastasis, chemotherapeutic response,

and aggressive pathological type. Multivariate regression analysis further showed that higher methylation levels were independently linked to increased rates of metastasis and more malignant pathological profiles. These collective findings suggest that *MSH6* methylation may serve as a potential biomarker for the diagnosis of RB. However, large-scale studies are still needed to validate these results.

Previous studies have shown diverse context-dependent functions for *MSH6* across different tumor types. For example, reduced MSH6 protein expression is associated with recurrence in glioblastoma[26], while its overexpression may indicate aggressiveness in prostate cancer[21]. Conversely, certain *MSH6* mutations in advanced prostate cancer are linked to better responses to hormonal agents and immunotherapies[27]. In microsatellite unstable colorectal cancer, loss of MSH6 protein demonstrates predilection for male patients, colonic tumor location, and poorly differentiated histology[22].

In our study, we observed that *MSH6* transcription was downregulated in RB tissues compared to controls, particularly in samples with higher methylation levels. In addition to mRNA analysis, we performed a preliminary Western blot experiment to assess MSH6 protein expression in one pair of RB and control tissues. This individual case suggested that MSH6 protein levels decreased in RB, in line with the observed downregulation at the mRNA level and increased promoter methylation. However, as only one case was analyzed, this result should be interpreted with great caution and cannot be generalized. Although our results suggest that promoter methylation may conceivably contribute to reduced *MSH6* expression in RB, alternative regulatory mechanisms, including mutations and allele deletions, remain plausible modulators of gene expression. Our findings are consistent with reports in pituitary neuroendocrine tumors and breast cancer[20,24-25,28-29], yet diverges from observations in colorectal and endometrial malignancies where distinct mechanisms may predominate[22,30]. Further studies with larger sample sets remain needed to validate these findings and to clarify the biological impact of *MSH6* loss in RB pathobiology.

Emerging evidence shows that *MSH6* loss exhibits context-dependent therapeutic implications, simultaneously driving chemoresistance while potentiating immunotherapy responses. In glioblastoma, temozolomide-induced *MSH6* mutations cause therapeutic resistance and disease recurrence. Experimental *MSH6* knockdown increases temozolomide resistance, whereas re-expression restores chemosensitivity. Conversely, in endometrial cancer, low *MSH6* levels are associated with increased immune infiltration, higher programmed death-ligand 1/2 expression, and better clinical responses to immune checkpoint inhibitors.

In light of our findings, demonstrating elevated *MSH6* methylation and decreased transcription in RB, it is plausible that epigenetic silencing of *MSH6* contributes to more aggressive tumor behavior and reduced chemotherapeutic efficacy. Simultaneously, such epigenetically altered tumors may exhibit differential responses to immunotherapy. These mechanistically distinct hypotheses require rigorous validation in integrated RB models, incorporating clinicopathological correlation with invasion/metastasis indices, survival analyses, and functional assessments of treatment sensitivity profiles.

Our ROC curve analysis demonstrated that *MSH6* gene methylation levels had good diagnostic value for RB, with an AUC of 0.847, sensitivity of 78.43%, and specificity of 80.65%. These data indicate that *MSH6* methylation may serve as a clinically promising biomarker for early detection of RB. Moreover, quantitative assessment of *MSH6* methylation status could help identify new therapeutic targets and inform the development of personalized treatment strategies for affected patients.

This study still has several limitations. Our study was conducted at a single center, which may limit the representativeness and generalizability of the results. Patient populations from different geographic regions or with varied genetic backgrounds may exhibit different clinical and molecular characteristics. Therefore, caution should be exercised when extrapolating our findings to other populations. Second, methylation analysis was performed using qPCR and MSP, without large-scale whole-genome methylation profiling. As a result, some methylation sites may have been missed. In future work, we plan to conduct multi-center studies with larger cohorts and to use broader methylation analysis to validate and extend our results.

In conclusion, collectively, this study suggests that the methylation level of the *MSH6* gene plays a significant role in the onset and progression of RB, exhibiting strong clinicopathological correlations and diagnostic value. These findings open up new avenues for research directions and clinical applications, particularly in early diagnosis, prognostic evaluation, and targeted therapies for RB.

ACKNOWLEDGEMENTS

Authors' Contributions: Zhang CF wrote the main manuscript text; Zhao L conduct statistical analysis; Jian TM perform table production; Guo YF designed the subject. All authors reviewed the manuscript.

Data Availability: Data are available from the corresponding author under sound reasoning.

Conflicts of Interest: Zhang CF, None; **Zhao L,** None; **Jian TM,** None; **Guo YF,** None.

REFERENCES

1 Li C, Zhang L, Zhang J, *et al*. Global, regional and national burden due to retinoblastoma in children aged younger than 10 years from 1990 to

2021. *BMC Med* 2024;22(1):604.

2 Bilbeisi T, Almasry R, Obeidat M, *et al*. Causes of death and survival analysis for patients with retinoblastoma in Jordan. *Front Med (Lausanne)* 2023;10:1244308.

3 Li N, Wang YZ, Zhang Y, *et al*. Characteristics of patients with recurrent retinoblastoma: a survival analysis. *BMC Cancer* 2024;24(1):287.

4 Norrie JL, Nityanandam A, Lai K, *et al*. Retinoblastoma from human stem cell-derived retinal organoids. *Nat Commun* 2021;12(1):4535.

5 Li HT, Xu L, Weisenberger DJ, *et al*. Characterizing DNA methylation signatures of retinoblastoma using aqueous humor liquid biopsy. *Nat Commun* 2022;13(1):5523.

6 Yamada Y, Venkadakrishnan VB, Mizuno K, *et al*. Targeting DNA methylation and B7-H3 in RB1-deficient and neuroendocrine prostate cancer. *Sci Transl Med* 2023;15(722):eadf6732.

7 Bonadona V, Bonaiti B, Olschwang S, *et al*. Cancer risks associated with germline mutations in MLH1, MSH2, and MSH6 genes in Lynch syndrome. *JAMA* 2011;305(22):2304-2310.

8 Chen W, Pearlman R, Hampel H, *et al*. MSH6 immunohistochemical heterogeneity in colorectal cancer: comparative sequencing from different tumor areas. *Hum Pathol* 2020;96:104-111.

9 Varol A, Boulos JC, Jin C, *et al*. Inhibition of MSH6 augments the antineoplastic efficacy of cisplatin in non-small cell lung cancer as autophagy modulator. *Chem Biol Interact* 2024;402:111193.

10 Zhou LZ, Xiao HQ, Chen J. Mismatch repair gene MSH6 correlates with the prognosis, immune status and immune checkpoint inhibitors response of endometrial cancer. *Front Immunol* 2024;15:1302797.

11 Singh L, Chinnaswamy G, Meel R, *et al*. Epidemiology, Diagnosis and Genetics of Retinoblastoma: ICMR Consensus Guidelines. *Indian J Pediatr* 2024;91(11):1147-1156.

12 Peeler CE, Gonzalez E. Retinoblastoma. *N Engl J Med* 2022;386(25):2412.

13 Leon-Ruiz J, Espinal-Centeno A, Blilou I, *et al*. RETINOBLASTOMA-RELATED interactions with key factors of the RNA-directed DNA methylation (RdDM) pathway and its influence on root development. *Planta* 2023;257(6):105.

14 Cerretelli G, Ager A, Arends MJ, *et al*. Molecular pathology of Lynch syndrome. *J Pathol* 2020;250(5):518-531.

15 Guazzi M, Polese A, Fiorentini C, *et al*. Left ventricular performance and related haemodynamic changes in Prinzmetal's variant angina pectoris. *Br Heart J* 1971;33(1):84-94.

16 Lu C, Xie M, Wendl MC, *et al*. Patterns and functional implications of rare germline variants across 12 cancer types. *Nat Commun* 2015;6:10086.

17 Young LC, Keuling AM, Lai R, *et al*. The associated contributions of p53 and the DNA mismatch repair protein Msh6 to spontaneous tumorigenesis. *Carcinogenesis* 2007;28(10):2131-2138.

18 Indraccolo S, Lombardi G, Fassan M, *et al*. Genetic, epigenetic, and immunologic profiling of MMR-deficient relapsed glioblastoma. *Clin Cancer Res* 2019;25(6):1828-1837.

19 Bateman AC. DNA mismatch repair protein immunohistochemistry-an illustrated guide. *Histopathology* 2021;79(2):128-138.

20 Roberts ME, Jackson SA, Susswein LR, *et al*. MSH6 and PMS2 germline pathogenic variants implicated in Lynch syndrome are associated with breast cancer. *Genet Med* 2018;20(10):1167-1174.

21 Albero-Gonzalez R, Hernandez-Llodra S, Juanpere N, *et al*. Immunohistochemical expression of mismatch repair proteins (MSH2, MSH6, MLH1, and PMS2) in prostate cancer: correlation with grade groups (WHO 2016) and ERG and PTEN status. *Virchows Arch* 2019;475(2):223-231.

22 Arshita N, Lestari RV, Hutajulu SH, *et al*. The tendency of having MSH2 and MSH6 microsatellite instability among clinicopathological features in patients with colorectal cancer. *Asian Pac J Cancer Prev* 2018;19(11):3147-3152.

23 Mattei AL, Bailly N, Meissner A. DNA methylation: a historical perspective. *Trends Genet* 2022;38(7):676-707.

24 Garcia-Martinez A, Sottile J, Sanchez-Tejada L, *et al*. DNA methylation of tumor suppressor genes in pituitary neuroendocrine tumors. *J Clin Endocrinol Metab* 2019;104(4):1272-1282.

25 Moelans CB, Verschuur-Maes AH, van Diest PJ. Frequent promoter hypermethylation of BRCA2, CDH13, MSH6, PAX5, PAX6 and WT1 in ductal carcinoma in situ and invasive breast cancer. *J Pathol* 2011;225(2):222-231.

26 Felsberg J, Thon N, Eigenbrod S, *et al*. Promoter methylation and expression of MGMT and the DNA mismatch repair genes MLH1, MSH2, MSH6 and PMS2 in paired primary and recurrent glioblastomas. *Int J Cancer* 2011;129(3):659-670.

27 Antonarakis ES, Shaukat F, Isaacsson Velho P, *et al*. Clinical Features and Therapeutic Outcomes in Men with Advanced Prostate Cancer and DNA Mismatch Repair Gene Mutations. *Eur Urol* 2019;75(3):378-382.

28 Belakhoua S, Vasudevaraja V, Schroff C, *et al*. DNA methylation profiling of pituitary neuroendocrine tumors identifies distinct clinical and pathological subtypes based on epigenetic differentiation. *Neuro Oncol* 2025;27(9):2341-2354.

29 Nieto JA, Yamin MA, Goldberg ID, *et al*. An empirical biomarker-based calculator for cystic index in a model of autosomal recessive polycystic kidney disease-the Nieto-Narayan formula. *PLoS One* 2016;11(10):e0163063. Correction: An empirical biomarker-based calculator for cystic index in a model of autosomal recessive polycystic kidney disease-the Nieto-Narayan formula. *PLoS One* 2016;11(12):e0168319.

30 Kim J, Kong JK, Yang W, *et al*. DNA mismatch repair protein immunohistochemistry and MLH1 promotor methylation testing for practical molecular classification and the prediction of prognosis in endometrial cancer. *Cancers (Basel)* 2018;10(9):279.